Electronic Supplementary Material (ESI) for Sustainable Energy & Fuels.

In Situ Formation of Renewable Cellulose Hydrogel Electrolyte for High-performance Flexible All-Solid-State Asymmetric Supercapacitors

Hongfei Wang, Juan Wu, Jun Qiu, Kefu Zhang, Jingwen Shao, Lifeng Yan*

CAS Key Laboratory of Soft Matter Chemistry, Hefei National Laboratory for Physical Sciences at the Microscale, and Department of Chemical Physics, University of Science and Technology of China, Hefei, 230026, P.R.China

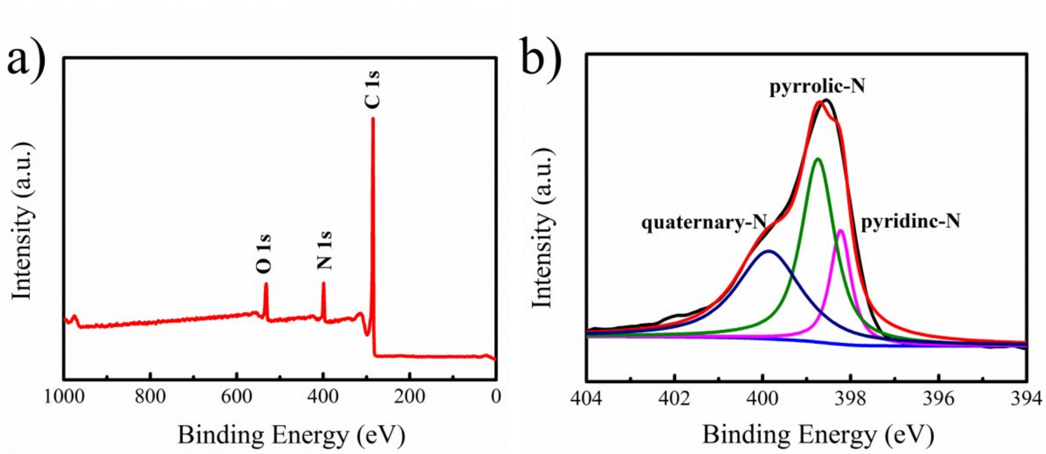

Figure S1. XPS survey spectra (a), N 1s pattern (b) of the NG sample.

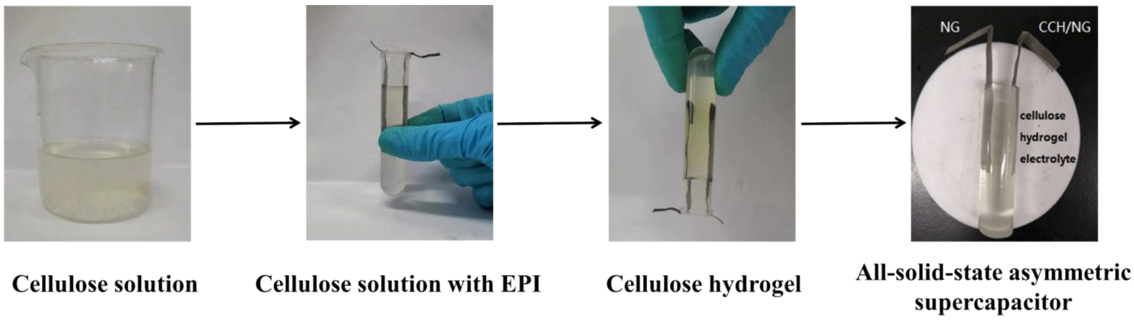

Figure S2. The optical image of the fabrication process of an all-solid-state hydrogel supercapacitor.

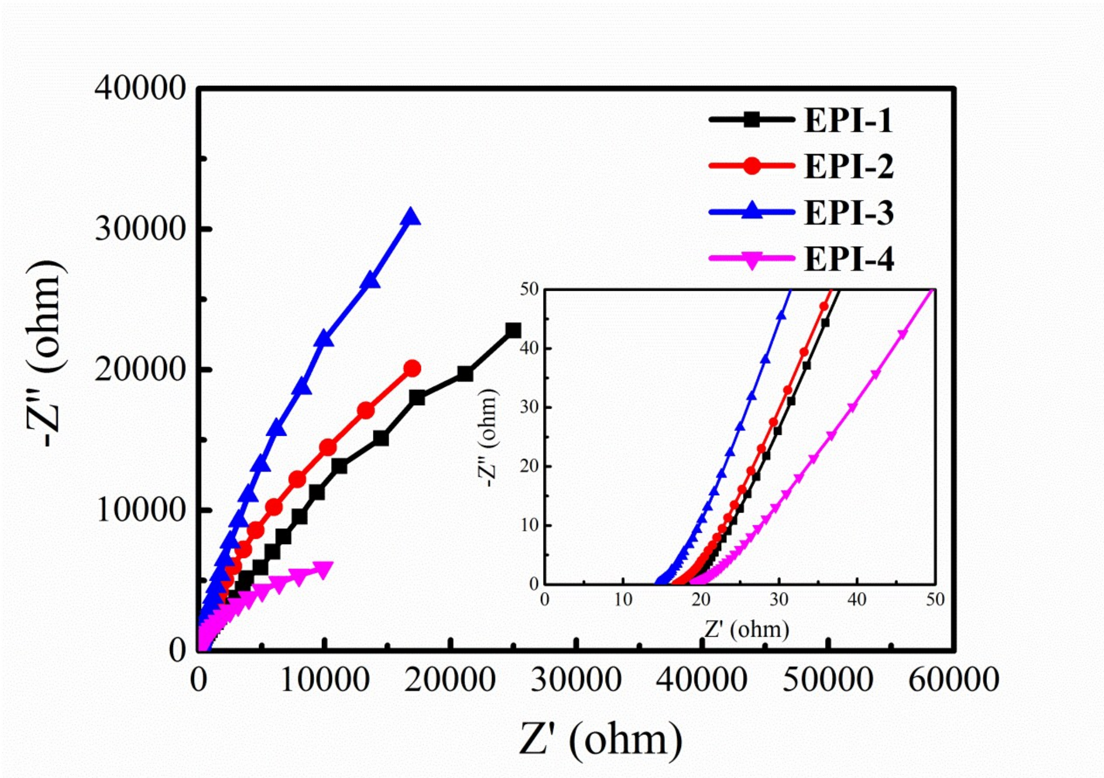

Figure S3. The frequency dependent impedance plots of the cellulose/NaOH hydrogel electrolytes with different EPI contents.

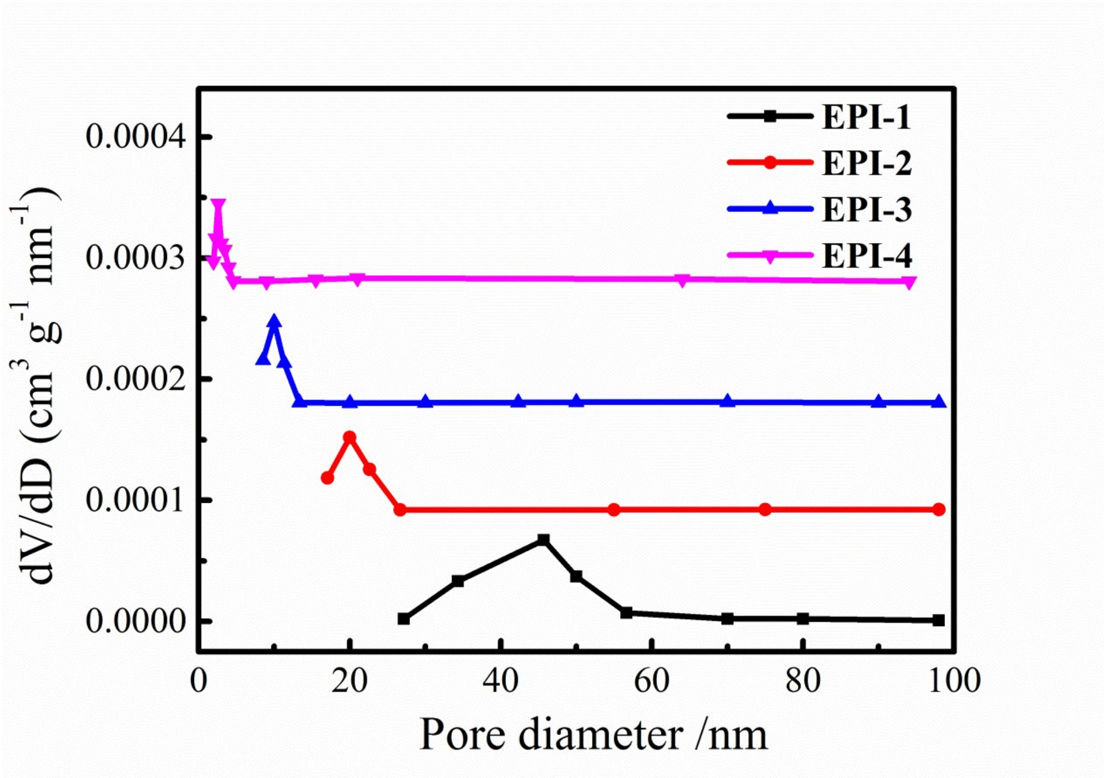

Figure S4. Pore size distribution for all cellulose/NaOH hydrogels with different contents of EPI.

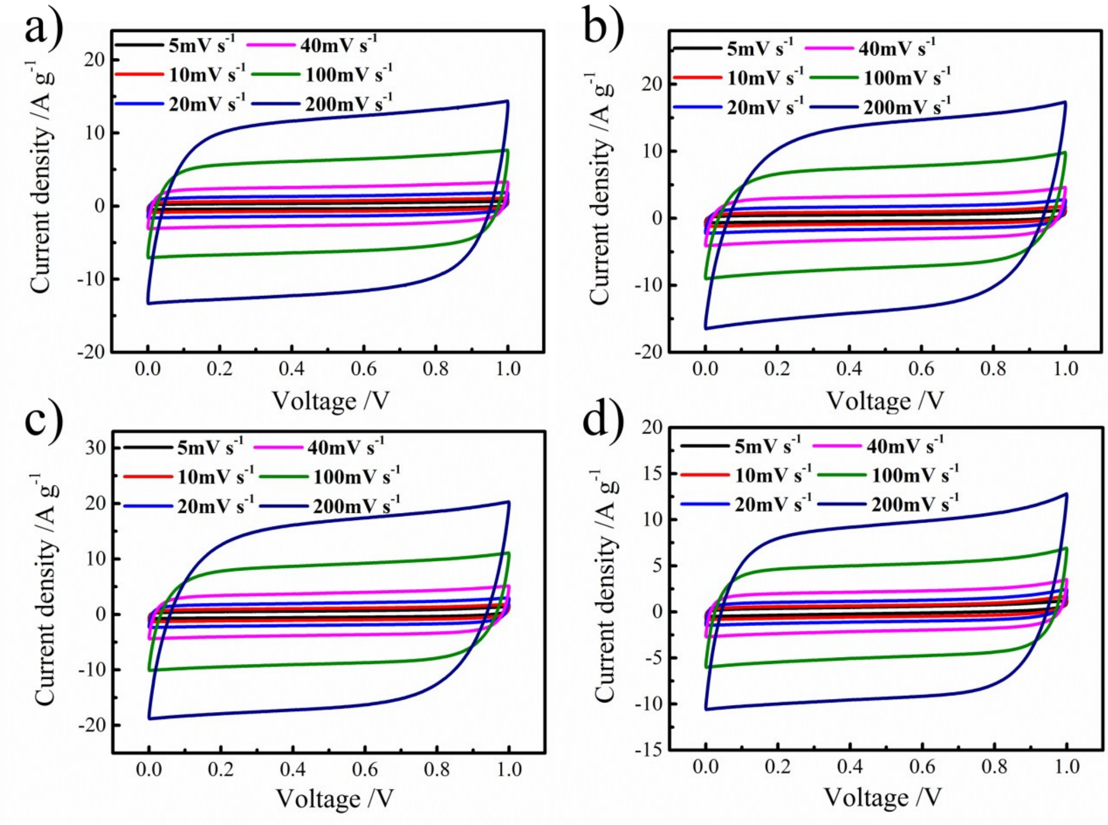

Figure S5. CV curves of the all-solid-state symmetric supercapacitors at the scan rates ranging from 5 mV s^{-1} to 200 mV s^{-1} using the electrolyte of cellulose/NaOH hydrogels with different contents of EPI. EPI-1 (a), EPI-2 (b), EPI-3 (c), EPI-4 (d).

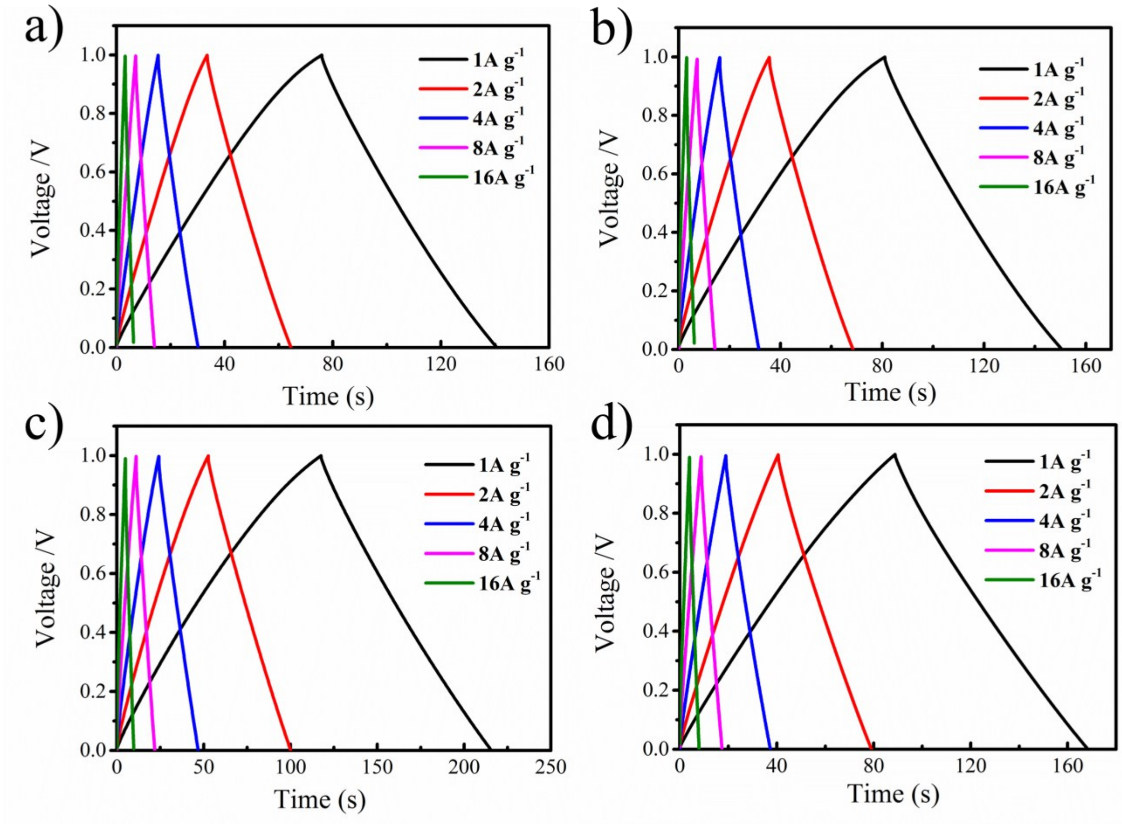

Figure S6. GCD profiles of the all-solid-state symmetric supercapacitors at the current densities ranging from 1 A g^{-1} to 16 A g^{-1} using the electrolyte of cellulose/NaOH hydrogels with different contents of EPI. EPI-1 (a), EPI-2 (b), EPI-3 (c), EPI-4 (d).

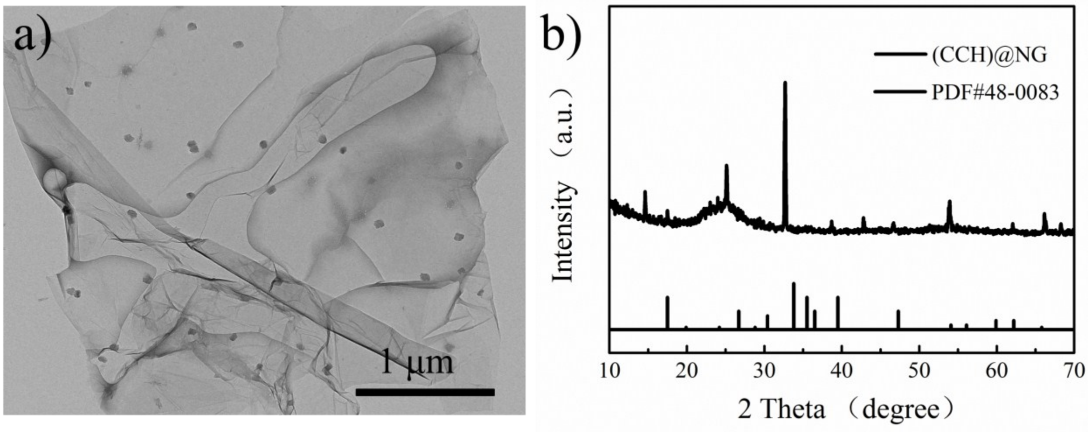

Figure S7. TEM (a) and XRD (b) pattern of the CCH/NG sample.

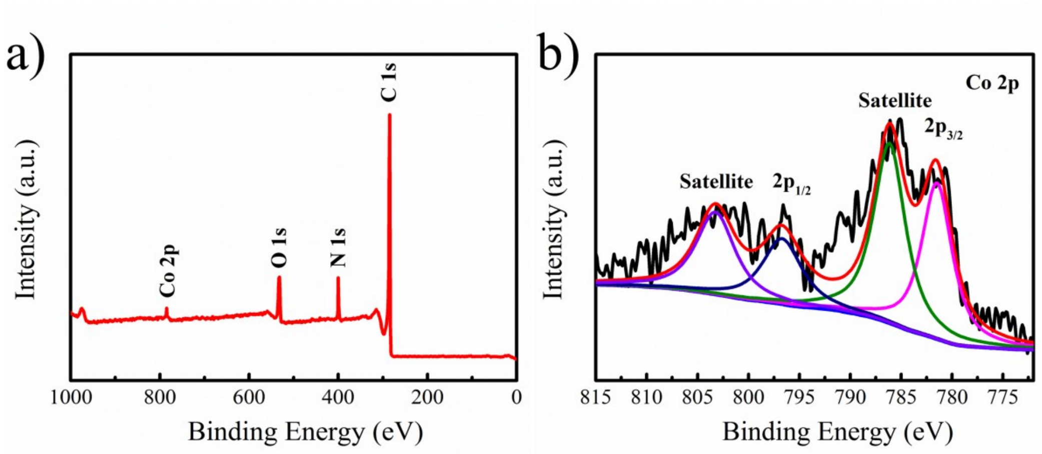

Figure S8. XPS survey spectra (a), Co 2p pattern (b) of the CCH/NG sample.

Table S1. Comparison of the presented supercapacitor with the previously-reported all-solid-state supercapacitors.

Electrode	Electrolyte	Specific capacitance	Energy density	Ref
CCH@NG ‖ NG	NaOH-cellulose	148F g^{-1} at 1.0 A g^{-1}	45.3Wh kg^{-1}	This work
MnO_2 film	NaCl-agarose	286.9 F g^{-1} at 0.5 A g^{-1}	25.5Wh kg^{-1}	S1
Activated carbon	[Bmim]Cl-cellulose	110 F g^{-1} at 1.0 A g^{-1}	4.37Wh kg^{-1}	S2
Activated carbon	H_3PO_4-PEG	64 F g^{-1} at 2 mV s^{-1}	------------	S3
Activated carbon	Li_2SO_4- carboxy methyl cellulose	174.8 F g^{-1} at 0.2 A g^{-1}	26.5Wh kg^{-1}	S4
m-LDH/NRG ‖ AC	KOH-PVA	56F g^{-1} at 0.2 A g^{-1}	19.9Wh kg^{-1}	S5
G/CoS_2/Ni_3S_4 ‖ GF	KOH-PVA	143.8 F g^{-1} at 0.5 A g^{-1}	44.9Wh kg^{-1}	S6
Activated carbon	Ionic liquid-PBI	85.5F g^{-1} at 0.1 A g^{-1}	11.8Wh kg^{-1}	S7
HPA-rGO	H_2SO_4-PVA	182.9F g^{-1} at 0.1 A g^{-1}	16.3Wh kg^{-1}	S8

Supporting references

[S1] W. G. Moon, G. P. Kim, M. Lee, H. D. Song and J. Yi, *Acs Appl Mater Inter*, 2015, **7**, 3503-3511.

[S2] D. W. Zhao, C. J. Chen, Q. Zhang, W. S. Chen, S. X. Liu, Q. W. Wang, Y. X. Liu, J. Li and H. P. Yu, *Adv Energy Mater*, 2017, **7**, 1700739.

[S3] Y. N. Sudhakar, D. K. Bhat and M. Selvakumar, *Polym Eng Sci*, 2016, **56**, 196-203.

[S4] J. Wei, J. Zhou, S. Su, J. Jiang, J. Feng and Q. Wang, *Chemsuschem*, 2018, **11**, 3410-3415.

[S5] Z. Dai, F. Liu, Y. Chen, Y. Liu, J. Bao and M. Han, *Nanoscale*, 2019, **11**, 9896-9905.

[S6] D. Jiang, H. Liang, W. Yang, Y. Liu, X. Cao, J. Zhang, C. Li, J. Liu and J. J. Gooding, *Carbon*, 2019, **146**, 557-567.

[S7] T. Mao, S. Wang, X. Wang, F. Liu, J. Li, H. Chen, D. Wang, G. Liu, J. Xu and Z. Wang, *Acs Appl Mater Inter*, 2019, **11**, 17742-17750.

[S8] C. Wu, T. Zhou, Y. Du, S. Dou, H. Zhang, L. Jiang and Q. Cheng, *Nano Energy*, 2019, 58, 517-527.